Progress In Electromagnetics Research, Vol. 141, 739–749, 2013

UNDERSTAND AND REALIZE AN "INVISIBLE GATEWAY" IN A CLASSICAL WAY

Xian Qi Lin[1,2,3], Yuan Jiang[3], Jun Ye Jin[3], Jia Wei Yu[3], and Sailing He[1,2,*]

[1]Department of Electromagnetic Engineering, Royal Institute of Technology (KTH), Stockholm 10044, Sweden

[2]JORCEP (Sino-Sweden Joint Research Center of Photonics), Zhejiang University, Hangzhou 310058, China

[3]EHF Key Lab of Fundamental Science, School of Electronic Engineering, University of Electronic Science and Technology of China, Chengdu 611731, China

Abstract—We create an invisible gateway simply by putting electric and magnetic superscatterers in a metallic waveguide. The characteristics of the electric and magnetic resonators are analyzed in a metallic hollow waveguide, and the dual-mode superscattering property is discussed in detail to broaden the bandwidth of the invisible gateway. Good agreement is achieved between the simulation and measurement for such an invisible gateway. The present work help readers understand easily how an invisible gateway works (or makes sense) in a classical way without using any complex metamaterial or complicated method of transformation optics.

1. INTRODUCTION

Invisibility technology has received great attention by both communities of science and engineering for centuries. Recently, the development on transformation optics [1–3] and electromagnetic (EM) metamaterials [4, 5] has paved a new way for making an object invisible. Using the transformation optics, different kinds of conceptual devices are proposed, such as invisible cloaks [6, 7], perfect lens [8, 9], and other illusion devices [10–12]. EM metamaterials are subwavelength-structured artificial materials with EM properties generally not found in nature.

Received 28 April 2013, Accepted 11 July 2013, Scheduled 9 August 2013
* Corresponding author: Sailing He (sailing@kth.se).

They provide the experimental foundation necessary to design the above-mentioned striking devices [13–15]. In 2009, Luo et al. [16] proposed the so-called “invisible gateway”, by which the light ray can be bounced back even though there is nothing on the light path through a physical gateway (or an “opened door”). The main design concept is to coat a negative index materials shell on a perfect electrical conductor to form a superscatterer (a scatterer bigger than its geometric size). While exact phase and field are restored in an invisibility cloak, such an “invisible gateway” just changes the reflection from zero to unity (without any requirement of phase restoration; consequently we believe an “invisible gateway” can be designed without the use of any fancy theory such as the transformation optics). Thus, word “invisible” in an “invisible gateway” (meaning the physical “gateway” exists but is invisible to electromagnetic waves, i.e., has the same reflection magnitude as the “background wall” so that the “gateway on the wall” becomes invisible to electromagnetic waves) has a different meaning from word “invisibility” in an “invisibility cloak”. Since then the “invisible gateway” has attracted much attention in the community. For example, Chen et al. [17] proposed another invisible gateway based on a magnetic photonic crystal structure and transformation optics. Using a transmission line medium, Li et al. [18] experimentally demonstrated the first invisible gateway. Other researches on invisible gateway realization have also been reported [19–21]. However, all of them are based on some complex metamaterials and the complicated method of transformation optics.

In this paper, we realize an “invisible gateway” in a simple and classical way without any complex media or transformation optics. We easily create an “invisible gateway” by putting electric and magnetic superscatterers in a metallic waveguide. The characteristics of electric and magnetic resonators are analyzed in a metallic hollow waveguide, and the superscattering property is discussed in detail. One sample for such a classical “invisible gateway” is fabricated and the measured results agree well with the simulated results. Such an invisible gateway makes easy sense to readers (as compared with the fancy “invisible gateway” based on metamaterials and transformation), and this is the main purpose of the present paper (instead of claiming anything fancy, new or surprising).

2. A WAVEGUIDE MODEL FOR “INVISIBLE GATEWAY”

A metal hollow waveguide structure is presented in Fig. 1 with the gate sizes of $a = 14.24\,\mathrm{mm}$ and $b = 7.12\,\mathrm{mm}$. The cutoff frequencies ($f_{c,mn}$)

of different propagation modes can be calculated as [22]

$$f_{c,mn} = \frac{c}{2\pi}\sqrt{\left(\frac{m\pi}{a}\right)^2 + \left(\frac{n\pi}{b}\right)^2}, \tag{1}$$

where c is the light speed in free space, and m and n correspond to the number of half-wave variations of the field in x and y directions, respectively. From Eq. (1), we can obtain $f_{c,mn}$ for the first few values of m and n as shown in Table 1. The typical E-field distributions of these propagation modes are illustrated in Fig. 1. Different resonances can be excited by variously inserted structures and input modes. Take TE_{10} mode for example, a metal strip line inserted in the centrally E-plane (as shown in the subfigure in Fig. 2(a)) can easily produce a strong electric resonance. Here we use a high frequency structure simulator (HFSS) to obtain the resonant characteristics. The simulated reflectance ($|R|$) and transmittance ($|T|$) are presented in Fig. 2(a) with $t = 0.018$ mm, $w_1 = 0.2$ mm and $l_1 = 3.0$ mm,

Table 1. $f_{c,mn}$ for the first few values of m and n.

Mode	TE	TE	TE	TE, TM	TE, TM
m	1	2	0	1	2
n	0	0	1	1	1
$f_{c,mn}$	10.53	21.07	21.07	23.55	29.79

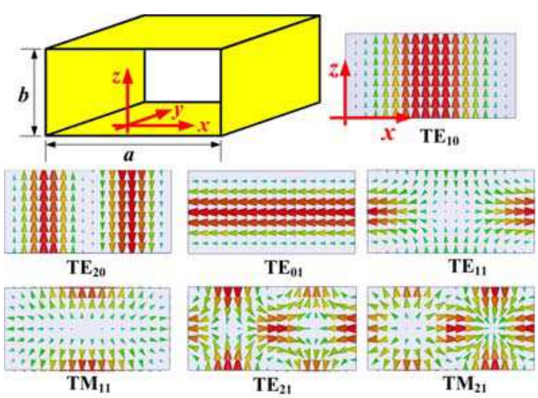

Figure 1. Schematic structure of a hollow waveguide and E-field distributions of first few propagation modes with $a = 14.24$ mm and $b = 7.12$ mm.

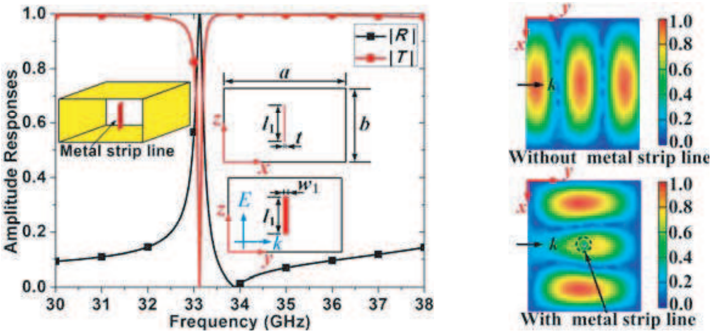

(a) Simulated $|R|$ and $|T|$ (b) E distributions

Figure 2. Schematic structures and resonant responses of a metal strip line inserted in a hollow waveguide with $a = 14.24\,\mathrm{mm}$, $b = 7.12\,\mathrm{mm}$, $t = 0.018\,\mathrm{mm}$, $w_1 = 0.2\,\mathrm{mm}$ and $l_1 = 3.0\,\mathrm{mm}$.

where a stop band is obtained near 33.12 GHz. Different amplitude distributions of the E-field in the central H-plane at 33.12 GHz are compared in Fig. 2(b), from which we easily observe that the original electromagnetic propagation through the gate area of $14.24\,\mathrm{mm} \times 7.12\,\mathrm{mm}$ is perfectly blocked by the inserted metal strip line with its cross section area of $0.018\,\mathrm{mm} \times 3.0\,\mathrm{mm}$ (only about 0.053% of the gate area). Superscattering of the metal strip line at its resonant frequency band is presented.

As illustrated in Fig. 1, all the z-components of the total E-field of these propagation modes presented in Table 1 (except for TE_{10}) are near zero at the central place, and no resonance can be excited by such a centrally inserted metal strip line. In order to block more modes of the input wave, the metal strip line should be moved to the side of the waveguide. Such movement also meets the requirements of an invisible gateway. We consider a simple translation with a displacement of $l_x = 2\,\mathrm{mm}$ as shown in the subfigure in Fig. 3(a). In this case, two resonances are excited by TE_{10} and TE_{20} input modes, respectively. The simulated amplitude responses are presented in Fig. 3(a), where the two resonances have the same resonant frequency of 33.11 GHz but with different resonant bandwidth. The E- and H-directions of TE_{10} and TE_{20} input modes are the same and thus the resonant frequencies are identical regardless of the varied structures and different places. However, the amplitude of E-field at the place of $l_x = 2\,\mathrm{mm}$ in the TE_{20} mode is much larger than that in the TE_{10} mode. Stronger coupling between the strip line and input electromagnetic field are presented in the TE_{20} mode which finally leads to a wider resonant frequency-band. The bandwidth can be broadened further by, e.g., stitching together the frequencies of more resonating modes. However, this is not given here as it is not the main purpose of the present paper. We extract the amplitude distributions of the E-field in the central H-plane at 33.11 GHz and compare them in Fig. 3(b), from which we observe that superscattering of the metal strip line at its resonant frequency band is achieved once again if excited by either the TE_{10} or TE_{20} input mode. These superscatterers make the metallic waveguide ("gateway") invisible (all reflected as if the gateway does not exist) to these guided modes (a typical analogue to plane waves in free space, as often made in literature), though the "gateway" is still widely opened (as the superscatterers are just on the walls). It is worth mentioning that such superscattering can also be obtained even when the metal strip line is placed in free space and excited by the TEM input mode (certainly the resonance frequencies may change).

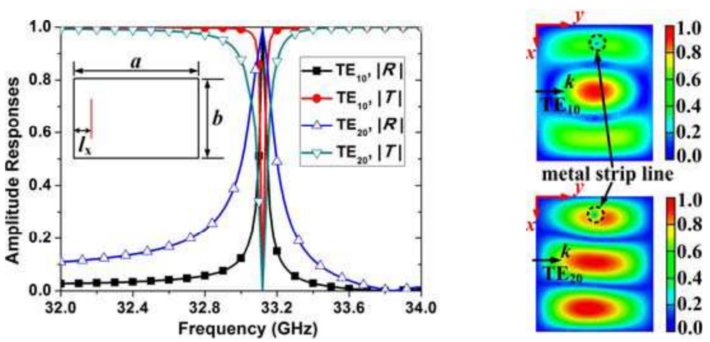

(a) Simulated $|R|$ and $|T|$ (b) $|E|$ distributions

Figure 3. Schematic structures and resonant responses of a metal strip line excited by the TE_{10} and TE_{20} input modes.

3. EXPERIMENTAL RESULTS

Now we set up a related experiment to validate the above superscattering performance. Taking a standard Ka-band waveguide ($a_{in} = 7.12$ mm and $b_{in} = 3.56$ mm) for the input/output connector, the experimental schematic structures are presented in Fig. 4(a). Two linear gradual transitions from the standard Ka-band waveguide (7.12 mm $\times$ 3.56 mm) to the main gateway (7.12 mm $\times$ 7.12 mm) at input and output ports are designed for negligible effect on the superscattering. The area of the main gateway is reduced from 14.24 mm $\times$ 7.12 mm to 7.12 mm $\times$ 7.12 mm just for simplification in

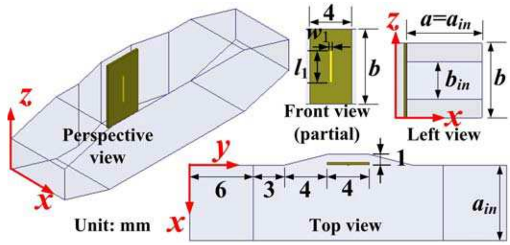

(a) Schematic structures

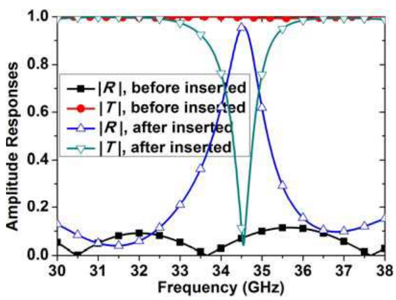

(b) Simulated $|R|$ and $|T|$

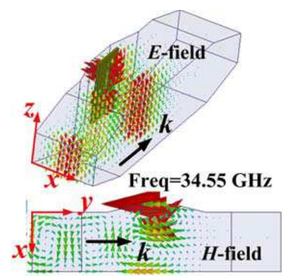

(c) E and H field distributions

Figure 4. Invisible gateway realized by an electric supperscatter.

measurement. In this situation, only the dominant mode of TE_{10} can be input into the waveguide. Extra space is added for placing the copper strip line fabricated on a Rogers 5880 substrate with thickness of 0.254 mm and relative permittivity of $\varepsilon_r = 2.2$ (loss tangent $\mathrm{tg}\delta = 0.0009$). The extra space only has a thickness of 1 mm in x-direction which is much smaller than that presented in Ref. [18]. The simulated results of reflectance and transmittance are presented in Fig. 4(b) where two cases of the waveguide respectively embedded with or without the superscatter (the electric resonator) are compared. After the superscatter is inserted into the waveguide, great blocking is achieved near 34.55 GHz. We illustrate the E and H field distributions at 34.55 GHz in Fig. 4(c), from which we see more clearly that an invisible gateway is obtained. Such an invisible gateway has a much simpler structure and is easy to realize and apply. However, the working frequency band is a bit narrow. Taking 90% blocking of the transmitted power (referred to $|T| = 0.33$) as the threshold value, the relative bandwidth is only 0.87% (from 34.39 GHz to 34.69 GHz). In order to use it in a practical application, the band must be widened. Here we introduce an additional magnetic superscatter to increase the bandwidth.

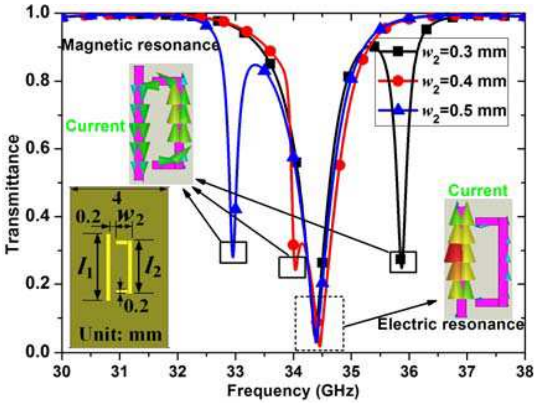

Figure 5. Schematic structure and simulated transmittance of dual-mode superscatter inserted in a metallic waveguide with fixed $l_2 = 2.4\,\text{mm}$ and varied $w_2 = 0.3$, 0.4, $0.5\,\text{mm}$.

The magnetic superscatter is realized by the structure composed of a reversed C-shaped structure and a strip line as shown in the subfigure in Fig. 5. By tuning the width (w_2) or length (l_2) of the reversed C-shaped structure, the magnetic resonant frequency can be varied. The relative simulated transmittance is given in Fig. 5 with fixed $l_2 = 2.4\,\text{mm}$ and varied $w_2 = 0.3$, 0.4, $0.5\,\text{mm}$. From the results, we found that interestingly the electric resonant frequency is nearly fixed at 34.45 GHz. This is because the electric resonance is mainly induced by the strip line and hardly affected by w_2. The magnetic resonant frequency can decrease easily when w_2 increases. The current distributions on the strip line and reversed C-shaped structure at the electric and magnetic resonant frequencies are also illustrated in Fig. 5, from which we observe that the current flows in linear direction at the electric resonant frequencies but in ring direction at the magnetic resonant frequencies. This further certifies that a dual-mode supperscatter is achieved in such an integrated structure. In order to get a flatter transition between the electric resonant band and magnetic resonant band, the value of w_2 is further optimized by using the HFSS. Finally, $w_2 = 0.395\,\text{mm}$ is used in the fabrication.

The photographs of the fabricated sample are presented in Fig. 6(a). Its reflection and transmission responses were measured by using Agilent 8757D Scalar Network Analyzer and compared with the simulated results as shown in Fig. 6(b). Good agreement between simulation and measurement is achieved. The simulated frequency band of larger than 90% power blocking ($|T| = 0.33$) is from 34.10 GHz

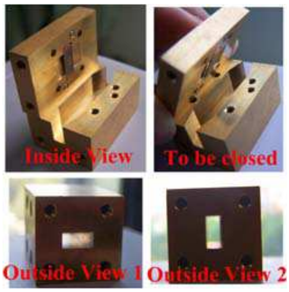

(a) Photographs

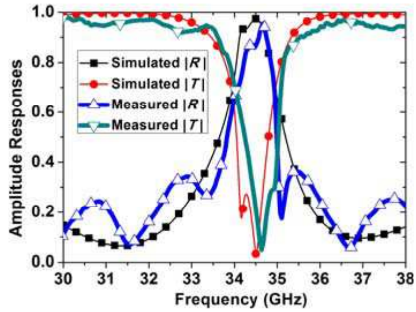

(b) $|R|$ and $|T|$

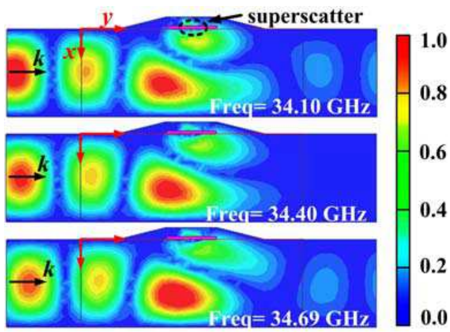

(c) simulated $|E|$ distributions in the central H-plane

Figure 6. Photographs and amplitude responses of fabricated invisible gateway.

to 34.69 GHz with relative band width of 1.72%, while the measured frequency band of larger than 90% power blocking is from 34.40 GHz to 34.97 GHz with relative bandwidth of 1.64%. Slightly frequency shifting is caused mainly by the fabricated error of the print circuit and the metallic waveguide. Limited by the measurement, we only illustrate the simulated $|E|$ distributions in the central H-plane at different frequencies in Fig. 6(c), from which we see more clearly that the invisible gateway works well from 34.10 GHz and 34.69 GHz. If needed, the superscattering bandwidth can be further broadened by cascading more unit cells of such a dual-mode superscatter.

It is worth mentioning that such a supperscatter will perform much better under the exciting of the TE_{20} mode where stronger coupling between the supperscatter and the TE_{20} input field will be presented. In addition, the proposed dual-mode superscatter can block more propagation modes.

4. CONCLUSION

To summarize, we have re-analyzed the characteristics of an electric resonator in a metal hollow waveguide. Using such an electric superscatter, an invisible gateway has been realized (i.e., the gateway exists physically but is invisible to the incident electromagnetic wave). In order to broaden the bandwidth of the invisible gateway, a magnetic superscatter has been further integrated with the electric superscatter. By using such a dual-mode superscatter, the invisible gateway has been finally designed and fabricated. Good agreement between simulation and measurement has been achieved. The superscattering bandwidth could be further broadened by cascading more unit cells of such a dual-mode superscatter. No complex metamaterials and complicated method of transformation optics are required in our invisible gateway design, and the size is much more compact than the other invisible gateways reported. The present work help readers understand easily how an invisible gateway works and makes a good sense in a classical way. Then what is the advantage of the original invisible gateway based on metamaterials and transformation optics? Well, at least one advantage, namely, the invisible gateway based on metamaterials and transformation optics can be so large that a person can walk through (theoretically speaking, though difficult to realize due to the loss of metamaterials, etc.).

ACKNOWLEDGMENT

This work was partially supported by NSFC (Nos. 61178062, 60901022 and 60990322), the National High Technology Research and Development Program of China (2012AA030402), RFDP (No. 20090185120005), the Fundamental Research Funds for the Central Universities, Swedish VR grant (# 621-2011-4620) and AOARD.

REFERENCES

1. Leonhardt, U., "Optical conformal mapping," *Science*, Vol. 312, 1777–1780, 2006.
2. Pendry, J. B., D. Schurig, and D. R. Smith, "Controlling electromagnetic fields," *Science*, Vol. 23, 1780–1782, 2006.
3. Chen, H. Y., C. T. Chan, and P. Sheng, "Transformation optics and metamaterials," *Nature Mater.*, Vol. 9, 387–396, 2010.
4. Smith, D. R., W. J. Padilla, D. C. Vier, S. C. Nemat-Nasser, and S. Schultz, "Composite medium with simultaneously negative

permeability and permittivity," *Phys. Rev. Lett.*, Vol. 84, No. 18, 4184–4187, 2000.

5. Shelby, R. A., D. R. Smith, and S. Schultz, "Experimental verification of a negative index of refraction," *Science*, Vol. 292, No. 5514, 77–79, 2001.
6. Alù, A. and N. Engheta, "Achieving transparency with plasmonic and metamaterial coatings," *Phys. Rev. E*, Vol. 72, No. 016623, 2005.
7. Li, J. S. and J. B. Pendry, "Hiding under the carpet: A new strategy for cloaking," *Phys. Rev. Lett.*, Vol. 101, No. 203901, 2008.
8. Pendry, J. B., "Negative refraction makes a perfect lens," *Phys. Rev. Lett.*, Vol. 85, No. 3966, 2000.
9. Wee, W. H. and J. B. Pendry, "Universal evolution of perfect lenses," *Phys. Rev. Lett.*, Vol. 106, No. 165503, 2011.
10. Chen, H. Y. and C. T. Chan, "Transformation media that rotate electromagnetic fields," *Appl. Phys. Lett.*, Vol. 90, No. 241105, 2007.
11. Lai, Y., J. Ng, H. Y. Chen, D. Z. Han, J. J. Xiao, Z. Q. Zhang, and C. T. Chan, "Illusion optics: The optical transformation of an object into another object," *Phys. Rev. Lett.*, Vol. 102, No. 253902, 2009.
12. Yan, W., M. Yan, and M. Qiu, "Generalized nihility media from transformation optics," *Journal of Optics*, Vol. 13, No. 024005, 2011.
13. Rainwater, D., A. Kerkhoff, K. Melin, J. C. Soric, G. Moreno, and A. Alù, "Experimental verification of three-dimensional plasmonic cloaking in free-space," *New Journal of Physics*, Vol. 14, No. 013054, 2012.
14. Costa, J. T. and M. G. Silveirinha, "Mimicking the Veselago-Pendry lens with broadband matched double-negative metamaterials," *Phys. Rev. B*, Vol. 84, No. 155131, 2011.
15. Jiang, W. X. and T, J, Cui, "Radar illusion via metamaterials," *Phys. Rev. E*, Vol. 83, No. 026601, 2011.
16. Luo, X. D., T. Yang, Y. Gu, H. Y. Chen, and H. R. Ma, "Conceal an entrance by means of superscatterer," *Phys. Lett.*, Vol. 94, No. 223513, 2009.
17. Chen, H., C. T. Chan, S. Liu, and Z. Lin, "A simple route to a tunable electromagnetic gateway," *New J. Phys.*, Vol. 11, No. 083012, 2009.
18. Li, C., X. Meng, X. Liu, F. Li, G. Fang, H. Chen, and C. T. Chan,

"Experimental realization of a circuit-based broadband illusion-optics analogue," *Phys. Rev. Lett.*, Vol. 105, No. 233906, 2010.

19. Zhang, J. J., Y. Luo, H. S. Chen, J. Tao, H. Fu, B. Wu, L. X. Ran, and J. A. Kong, "Guiding waves through an invisible tunnel," *Optics Express*, Vol. 17, No. 8, 6203–6208, 2009.
20. Castaldi, G., I. Gallina, V. Galdi, A. Alù, and N. Engheta, "Power scattering and absorption mediated by cloak/anti-cloak interactions: A transformation-optics route toward invisible sensors," *J. Opt. Soc. Am. B*, Vol. 27, No. 10, 2132–2140, 2010.
21. Chen, Z. H., L. H. Wang, C. M. Wang, and Z. H. Fang, "General complementary media: Electromagnetically transforming a small rectangle object to a large convex/concave pentagon object," *Chinese Optics Letters*, Vol. 9, Issue 2, No. 021601, 2011.
22. Pozar, D. M., *Microwave Engineering*, 3rd edition, Wiley, New York, 2003.